Journal of Engineering, Project, and Production Management
2026, 16(5), 2025-337

Improving Spatiotemporal Accuracy of Port Air Quality Monitoring Using GCN-Att Fusion Model

Shoubo Zhang[1], Pingwei Zhou[2], Guannan Xu[3], Zongtao Mu[4], and Dong Wang[5]
[1] Deputy Manager and Safety Director, First Stevedoring Branch Company, SPG Rizhao Port Group Co., Ltd. 276800, China, E-mail: jdy7141319@163.com (corresponding author).
[2] Deputy Manager, First Stevedoring Branch Company, SPG Rizhao Port Group Co., Ltd. 276800, China, E-mail: zpw306@163.com
[3] Deputy Director, Technology Innovation Center, SPG Rizhao Port Group Co., Ltd. 276800, China, E-mail: xuguannan_rzg@163.com
[4] Deputy Department Manager, Technology Innovation Center, SPG Rizhao Port Group Co., Ltd. 276800, China, E-mail: qq909_long@163.com
[5] Executive Director, Shandong Port Technology Group Rizhao Co., Ltd. 276826, China, E-mail: wd521cmm@163.com

Project Management
Received December 16, 2025; revised January 29, 2026; accepted March 1, 2026
Available online June 17, 2026

Abstract: The contradiction between dynamic pollution events in ports and the assumption of a static graph structure leads to a significant decline in the prediction performance of existing Graph Convolutional Network-Attention (GCN-Att) models under abrupt change scenarios. To address this issue, this paper develops a dynamic topology-sensing mechanism that constructs a dynamic spatial adjacency matrix integrating ship Automatic Identification System (AIS) trajectories and real-time meteorological data. A real-time edge-weight update unit driven by abrupt change events is designed to enable the graph structure to adaptively respond to the pollution diffusion process. Experiments show that in ship berthing events, the Root Mean Square Error (RMSE) of $PM_{2.5}$ prediction is 4.21±0.63 $\mu g/m^3$, with an R^2 of 0.89±0.04. Under extreme weather conditions such as typhoons, the model response latency is reduced to 8.1 seconds; the data missing tolerance reaches 86%; the Mean Absolute Error (MAE) of $PM_{2.5}$ is only 4.7 $\mu g/m^3$, significantly outperforming existing methods and validating its high accuracy, low latency, and strong robustness.

Keywords: Spatiotemporal monitoring, port air quality, graph attention networks, dynamic topology adaptation.

DOI 10.32738/JEPPM-2025-337

1. Introduction

As pivotal hubs within global logistics networks, port operations exert a direct and profound impact on surrounding ecological systems and public health security (Tseng and Ng, 2021; Santos, 2025; Barberi et al., 2021). As international trade grows, air pollution from a high concentration of ships and heavy cargo activity in the port area has become increasingly serious (Garbatov and Georgiev, 2022; Tai and Wang, 2022; Kim et al., 2022). Air quality monitoring is an essential component of environmental management, but current strategies require technologies capable of precisely characterizing spatiotemporal pollutant diffusion processes (Ye and Geng, 2023; Campos et al., 2021; Sembiring et al., 2024). However, the presence of unique dynamics and pollution sources in ports causes air quality to exhibit nonlinearity and rapid change, which prevents traditional monitoring technologies from capturing these changes. This technical bottleneck constrains the scientific decision-making and precision control of port environmental management.

Graph neural networks, owing to their strongly connected spatial relationship modeling abilities, have emerged as a valuable and leading technical avenue within the environmental monitoring discipline (Han et al., 2022). In early research, convolutional neural networks were combined with a residual learning mechanism, showing a significant improvement in the predictive accuracy of standard air quality models. However, there was almost no ability to adapt to complicated topology structures (Shi et al., 2024; Benhaddi and Ouarzazi, 2021). As research continues, gated mechanisms are brought to bear on prediction with the idea that they can enhance predictive abilities through newfound modeling of temporal dynamics in trajectories, yet these architectures impose a substantially higher computational burden during the training phase (Wang et

al., 2024). The recently developed GCN-Att fusion model integrates graph convolution with attention mechanisms. It achieves superior performance in conventional prediction tasks and can capture both spatial dependence and temporal importance weights (Li et al., 2023; Liu et al., 2023). However, such methods are generally based on fixed spatial adjacency matrices, and their underlying assumption of "static topology" cannot reflect real-time migration and dynamic reconstruction of port pollution sources, leading to prediction inaccuracies in sudden scenarios, such as instantaneous ship emissions or extreme weather. This structural defect indicates that although the existing GCN-Att model is effective in stable environments, it struggles to adapt to the high dynamism of ports.

In response to the specific circumstances of ports, some studies have sought to introduce dynamic modeling approaches. Zhou et al. (2022) constructed a real-time measurement modeling system for ship emission factors, emphasizing the necessity of dynamically coupling ship operation status with pollution emissions. Pan et al. (2024) revealed the spatiotemporal heterogeneity of complex emissions in port areas through a high-density air quality sensor network, providing a data basis for refined mapping. On this basis, Li et al. (2024) analyzed the causes of multi-source pollution in Shanghai Port. Lee et al. (2021) used AIS data and the Density-Based Spatial Clustering of Applications with Noise (DBSCAN) algorithm to mine ship activity patterns to construct spatial correlations. However, existing dynamic map methods are still limited by two shortcomings: first, relying on preset concentration thresholds to adjust the connection relationship of stations makes it difficult to adapt to the rapid changes in port operation modes and meteorological conditions; second, although the sliding window mechanism can reflect historical dynamics, it applies a large computational overhead and response latency. More importantly, current research has not effectively integrated the synergistic effects of ship trajectory dynamics and meteorological fields on pollutant diffusion paths. As Motlagh et al. (2023) noted, multi-source heterogeneous sensing required collaborative modeling to accurately capture abrupt events. Although Geng et al. (2023) and Liu et al. (2021) have provided technical support for ship motion prediction and trajectory visualization, respectively. Transforming such dynamic information into the topological evolution mechanism of graph neural networks in real-time remains an unsolved problem.

This paper directly addresses the aforementioned core contradictions, proposing a paradigm shift from "static topology" to "dynamic topology". By constructing an adaptive adjacency matrix driven by ship AIS trajectories and real-time meteorological data and designing a real-time edge-weight update mechanism triggered by abrupt events, the online reconstruction of the port pollution diffusion process using graph structures is achieved. This method breaks the GCN-Att model's dependence on a fixed topology and, for the first time, internalizes the essential characteristics of dynamic port pollution into the model's topological evolution logic. This work directly addresses the three major challenges revealed in the introduction: inaccuracy, response latency, and insufficient robustness. It not only provides a new paradigm for intelligent port environmental monitoring but also opens up new avenues for applying dynamic graph neural networks in high-abrupt-change scenarios.

2. Method

The air quality monitoring in the port region presents a key dilemma: dynamic pollution events/sources, and static monitoring models, especially during sudden or abrupt event scenarios, such as instantaneous ship emissions, where traditional fixed topology models struggle to depict the spatiotemporal evolution of pollutants. This chapter introduces a novel dynamic topological sensing GCN-Att facility fusion model that addresses the unique challenge of monitoring accuracy in the port environment through adaptive graph construction and feature extraction mechanisms.

2.1. Multi-Source Driven Dynamic Topology Construction Mechanism

The topological relationship between each port monitoring station is dynamically influenced by both ship activity and prevailing meteorological conditions, making it difficult for traditional fixed-topology models to accurately reflect real-time daily pollution diffusion processes. By proposing a dynamic topology construction method based on multi-source data fusion, this study addresses the topology model for real-time multi-data coupling. First, ship AIS trajectories are combined with meteorological observation data to produce an adaptively constructed spatial adjacency matrix that describes real-time pollution.

First, the port monitoring network is defined as a graph structure $G_t=(V,E_t,A_t)$. Among them, V is the set of nodes of N monitoring stations. E_t is the set of edges at time t. $A_t \in R^{N\times N}$ is the dynamic spatial adjacency matrix. The element a_{ij}^t of the adjacency matrix is calculated using the Eq. (1) (Ren et al., 2023; Gu et al., 2023).

$$a_{ij}^t=\frac{1}{1+e^{-\alpha(d_{ij}-\beta)}}\cdot max(0,cos\ (\theta_{ij}-\omega_t))\cdot e^{-\gamma\cdot\delta_{ij}^t} \quad (1)$$

In Eq. (1), d_{ij} represents the Euclidean distance between stations I and j; θ_{ij} is the azimuth angle from station i to j; ω_t is the prevailing wind direction at time t; δ_{ij}^t represents the intensity of ship activity near station i at time t; α, β, and γ are adjustment parameters that control the distance attenuation rate, effective radius of influence, and intensity of ship activity influence, respectively.

To accurately reflect the impact of instantaneous ship emissions on pollutant diffusion, a ship trajectory influence factor ζ_{ij}^t is applied (Li et al., 2024; Jia et al., 2023).

$$\zeta_{ij}^t=\sum_{k\in S_t}\frac{E_k}{4\pi\kappa_a d_{ik}^2}\cdot I(\parallel p_k-p_i \parallel \le r_{max})\cdot max(0,cos\ (\theta_{ik}-\omega_t)) \quad (2)$$

In Eq. (2), S_t represents the set of ships within the port area at time t; E_k represents the estimated emission intensity of ship k; κ_a represents the atmospheric diffusion coefficient; p_k and p_i represent the position coordinates of ship k and station i, respectively; r_{max} represents the maximum radius of influence; $I(\cdot)$ represents the indicator function.

Based on the above calculations, the final dynamic spatial adjacency matrix A_t is obtained through normalization, providing an accurate spatial relationship representation basis for subsequent feature extraction.

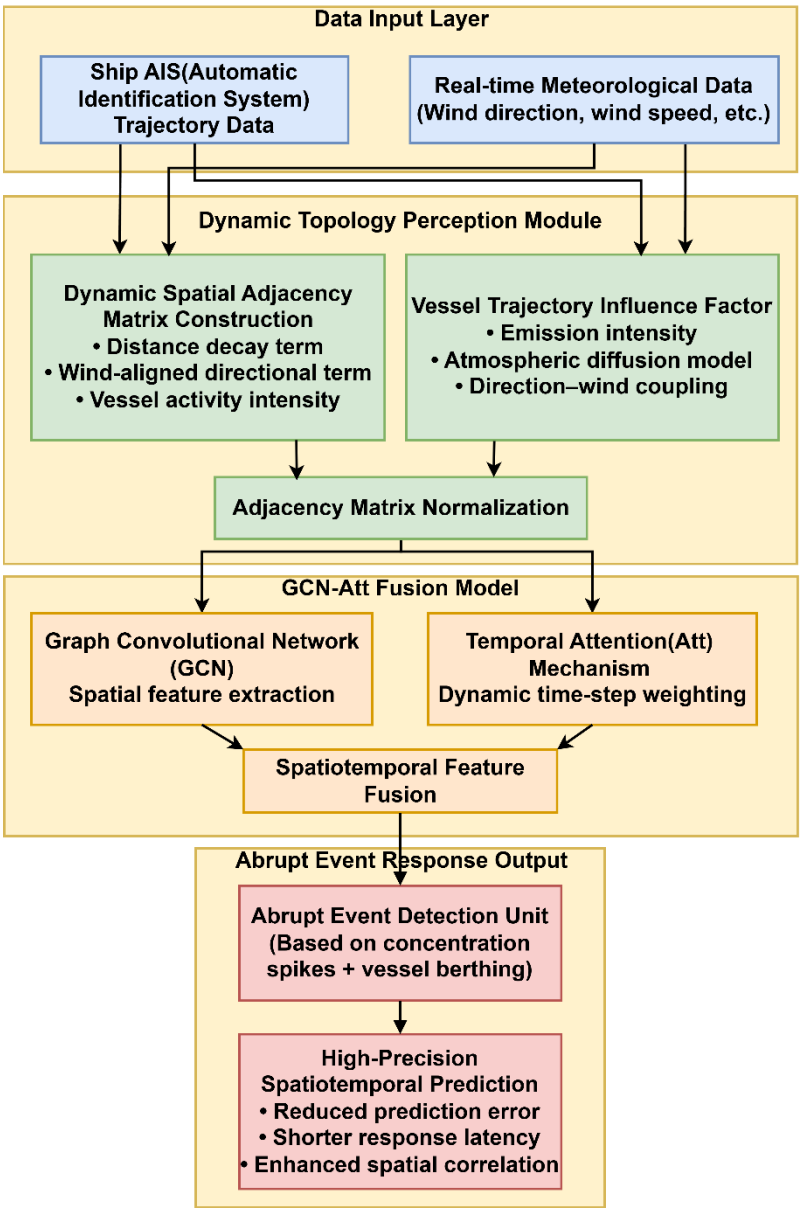

Fig. 1. Overall framework diagram of the model

Fig. 1 illustrates the overall framework of this study, presenting the complete technical process from AIS/meteorological data input, processing through the dynamic topology sensing module, to the final output of abrupt event prediction.

2.2. GCN-Att Spatiotemporal Feature Extraction Benchmark Model

Based on the dynamic topology A_t, an architecture combining a dual-channel graph convolutional network and a temporal attention mechanism is designed to systematically extract spatiotemporal features of port air quality. Considering the non-Euclidean spatial structure characteristics of port monitoring data, the spatial feature extraction channel uses a stacked two-layer graph convolutional layer processing (Malek, 2023; Pan et al., 2021).

$$H^{(l+1)}=\sigma\left(\hat{D}^{-\frac{1}{2}}\hat{A}\hat{D}^{-\frac{1}{2}}H^{(l)}\Theta^{(l)}\right) \tag{3}$$

In Eq. (3), $\hat{A}$ is the adjacency matrix with self-loops. $\hat{D}$ is the corresponding degree matrix, and its diagonal elements are $\hat{d}_{ii}=\sum_j \hat{a}_{ij}$; $H^{(l)}\in R^{N\times F_l}$ is the node feature matrix of the l-th layer; $\Theta^{(l)}\in R^{F_l\times F_{l+1}}$ is the learnable parameter matrix; $\sigma(\cdot)$ is the ReLU activation function; F_l represents the feature dimension of the l-th layer.

The temporal feature extraction channel employs a multi-head self-attention mechanism to dynamically assign weights to historical monitoring sequences (Wang et al., 2024; Jun et al., 2023).

$$\text{Attn}(Q,K,V)=\text{softmax}\left(\frac{QK^{\top}}{\sqrt{d_k}}+M\right)V \tag{4}$$

In Eq. (4), Q, K, and V are the query, key, and value vectors, respectively; $\top$ is the time step, d_k is the dimension of the key vector. $M\in R^{T\times T}$ is the mask matrix used to prevent future information leakage.

The fusion of spatial and temporal features provides a key basis for the subsequent detection of abrupt events, enabling the model to accurately identify dynamic pollution events in the port environment.

2.3. Mutation Event-Driven Dynamic Topology Adaptive Update Mechanism

Based on the features extracted in Section 2.2, a mutation event detection unit is designed to capture potential contamination mutations (Johnson et al., 2024).

$$\Psi_t(i)=\frac{1}{W}\sum_{\tau=t-W+1}^{t} I\left(\left|c_\tau(i)-\mu_{\tau\text{-}w}(i)\right|>\epsilon\cdot\sigma_{\tau\text{-}w}(i)\right)+\lambda\cdot I(v_{ship}(t,i)<v_{th}) \tag{5}$$

In Eq. (5), $c_\tau(i)$ is the pollutant concentration at station i at time τ, $\mu_{\tau\text{-}w}(i)$ and $\sigma_{\tau\text{-}w}(i)$ represent the mean and standard deviation within the sliding window $[\tau-w,\tau-1]$, respectively, ϵ represents the anomaly detection threshold, $v_{ship}(t,i)$ represents the average speed of ships near station i at time t, v_{th} represents the berthing determination threshold. W and w represent the short-term and long-term sliding window sizes, respectively, λ represents the ship activity weighting coefficient.

When $\Psi_t(i)>\psi_{th}$, a mutation event is determined to have occurred near station i, triggering a topology update. The edge weight update algorithm dynamically adjusts the graph structure based on the characteristics of the mutation event (Li, 2024; Islam et al., 2024).

$$\Delta A_t=\rho\cdot E_t\odot F_t\odot(1-A_t)\cdot e^{-\kappa(t-t_{event})} \tag{6}$$

In Eq. (6), $E_t\in R^{N\times N}$ is the event impact matrix; $F_t\in R^{N\times N}$ is the wind direction impact matrix; ρ is the update intensity coefficient; κ is the time decay rate; t_{event} is the event occurrence time.

The final dynamic topology update rule is (Liang et al., 2022).

$$A_{t+1}=A_t+\Delta A_t-\gamma_{stab}\cdot(A_t\odot(A_t>\tau_{conn})) \tag{7}$$

In Eq. (7), γ_{stab} is the structural stability coefficient; τ_{conn} is the connection strength threshold, used to prevent excessive density of the graph structure. Table 1 lists the core parameter configurations of this mechanism.

Table 1. Core parameters of the model

Parameter Name	Symbol	Value	Description
Anomaly detection threshold	ϵ	0.15	For concentration spike detection in Eq. (5)
Event trigger threshold	ψ_{th}	1.2	Composite score to activate topology update
Berthing determination threshold	v_{th}	2.3	Knots; identifies vessel docking Eq. (5)
Update intensity coefficient	ρ	0.42	Scales ΔA_t in dynamic adjacency update Eq. (6)
Structural stability coefficient	γ_{stab}	0.05	Prevents over-dense graph connections Eq. (7)

2.4. Multi-Task Loss Optimization Strategy

To balance the prediction accuracy and topological stability of the model in the mutation scenario, a dual-objective joint optimization framework is designed. The prediction error loss is weighted to highlight the prediction accuracy during the mutation event (Sun et al., 2022).

$$L_p=\frac{1}{N\cdot T}\sum_{i=1}^{N}\sum_{t=1}^{T}\omega_t\cdot l(\hat{y}_{i,t},y_{i,t}),\omega_t=1+\mu\cdot I(\Psi_t>\psi_{th}) \tag{8}$$

In Eq. (8), L_p is the weighted prediction error loss; $\hat{y}_{i,t}$ and $y_{i,t}$ are the predicted value and the true value, respectively. $l(\cdot,\cdot)$ is the Huber loss function, ω_t is the time weight, μ is the weight coefficient of the sudden event.

Topological stability loss is measured by calculating the Frobenius norm of the structural changes in the inter-step graph over continuous time:

$$L_s=\frac{1}{N^2}\sum_{t=2}^{T}\ //A_t-A_{t-1}//_F^2+\nu\cdot\text{Reg}(A_t) \tag{9}$$

In Eq. (9), $//\cdot//_F$ is the Frobenius norm. $\text{Reg}(A_t)$ is the graph sparsity regularization term, and ν is the sparsity coefficient.

The two loss terms are balanced using adaptive weighting coefficients to form the final optimization objective:

$$L_{total}=\xi(t)\cdot L_p+(1-\xi(t))\cdot L_s,\xi(t)=0.3+0.4\cdot\min\left(1,\frac{t}{T_{warm}}\right) \quad (10)$$

In Eq. (10), $\xi(t)$ is the prediction error loss weight; T_{warm} is the warm-up period, set to 50; t is the current training step number. The model training uses the AdamW optimizer, with an initial learning rate of 0.001, a weight decay coefficient of 0.01, and a batch size of 32, and gradient clipping is implemented to prevent gradient explosion. The experimental evaluation utilizes a multi-modal dataset comprising air quality station readings, meteorological tower observations, and vessel AIS logs collected from the target port area. Data preprocessing involved temporally aligning heterogeneous streams to a synchronized five-minute resolution and spatially mapping vessel coordinates to the monitoring network grid. The dataset is partitioned chronologically, with the initial portion used for training and the subsequent segment reserved for testing to strictly evaluate temporal generalization. Input features underwent Z-score normalization to accelerate convergence during the gradient descent optimization process.

3. Result

3.1. Quantification of the Prediction Accuracy of Mutation Events

Five periods of concentrated ship berthing are selected as test cases. Monitoring data for key pollutants, such as Particulate Matter $\leqslant$ 2.5 μm ($PM_{2.5}$) and Nitrogen Oxides (NO_x), are collected. RMSE, MAE, Mean Absolute Percentage Error (MAPE), Coefficient of Determination (R^2). The F1-score is calculated between the model's predicted and actual values. For each abrupt change event, a ±15-minute time window is set, and the trend of prediction error changes before and after the abrupt change point is statistically analyzed. The prediction error values of each monitoring station are marked on the port plan. The prediction performance for ship berthing events is visualized in Fig. 2, and the statistical results of each indicator are shown in Table 2.

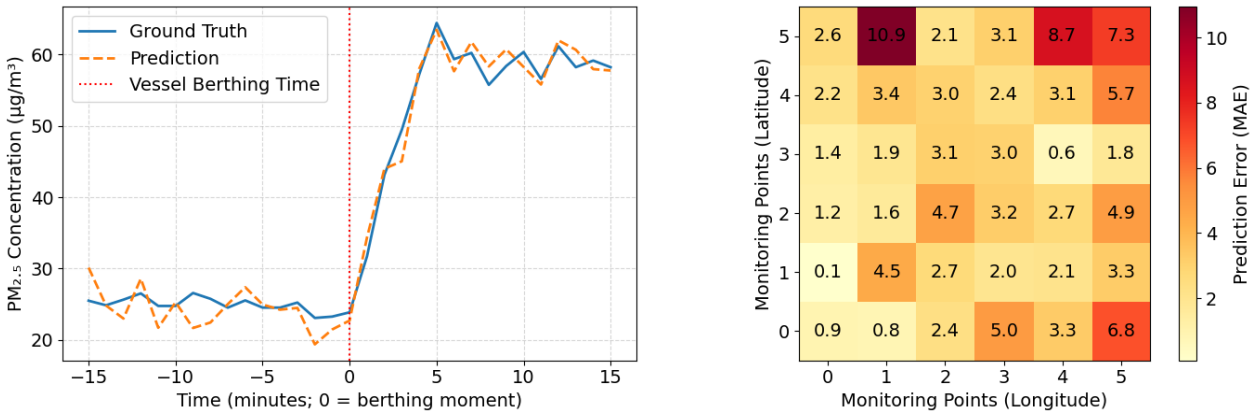

(a) Time-series predictions at abrupt change points (b) Thermal map of spatial prediction errors

Fig. 2. Visualization of prediction performance under ship berthing events

Table 2. Model prediction performance indicators under ship berthing events

Pollutants	RMSE (μg/m³)	MAE	MAPE (%)	R^2	F1-score
$PM_{2.5}$	4.21 ± 0.63	3.15 ± 0.48	12.7 ± 2.1	0.89 ± 0.04	0.84 ± 0.05
NO_x	6.84 ± 1.02	5.03 ± 0.76	15.3 ± 2.8	0.85 ± 0.05	0.79 ± 0.06

Fig. 2 illustrates the model's predictive performance during abrupt ship berthing events. Fig. 2(a) presents a time-series comparison curve of $PM_{2.5}$ concentration within a ±15-minute window (horizontal axis: time, vertical axis: concentration, unit: μg/m³). The actual value shows a significant jump at the berthing moment (t=0), while the predicted curve closely tracks this abrupt change, with only a slight lag after the peak. Fig. 2(b) uses the port plane as a base map and maps the mean absolute error for each station through a heat map. High error values are concentrated around the berths, while stations far from the operating area generally have lower errors, indicating that the model has a good ability to characterize the spatial heterogeneity of pollution diffusion.

Table 2 quantifies the overall performance under five berthing events: $PM_{2.5}$'s RMSE is 4.21±0.63 μg/m³. MAE is 3.15±0.48 μg/m³; MAPE is 12.7%±2.1%; R^2 reaches 0.89±0.04. The F1-score is 0.84±0.05. The NO_x index is generally robust. The low standard deviation reflects the model's consistent performance across different events, while the F1-score

demonstrates its effective ability to identify high-pollution states, validating the synergistic optimization effect of the dual objectives of regression and classification.

The above results stem from the dynamic topology sensing mechanism at the model's core: by fusing AIS trajectory and wind direction data, the edge weights of the adjacency matrix are updated in real time, enhancing the connection strength between the pollution source and downwind stations when abrupt changes occur in the graph structure, thereby guiding GCN-Att to accurately propagate instantaneous emission signals. This not only explains the rapid response and spatial error focusing phenomena in Fig. 2, but also supports the systematic improvement of various indicators in Table 2, fundamentally alleviating the modelling mismatch problem of static GCN-Att in dynamic pollution scenarios at ports.

3.2. Spatiotemporal Representation Efficiency of Dynamic Topological Mechanisms

The graph structure changes at each time step during model execution are recorded, and the correspondence between edge weight update frequency and ship activity events is statistically analysed. Static and dynamic topology models are run under the same input conditions, and the attention weight distributions of the two models are extracted and compared. For critical periods of abrupt events such as ship berthing, the change in the dynamic topology mechanism's ability to represent spatial correlations is analysed. The results are shown in Fig. 3.

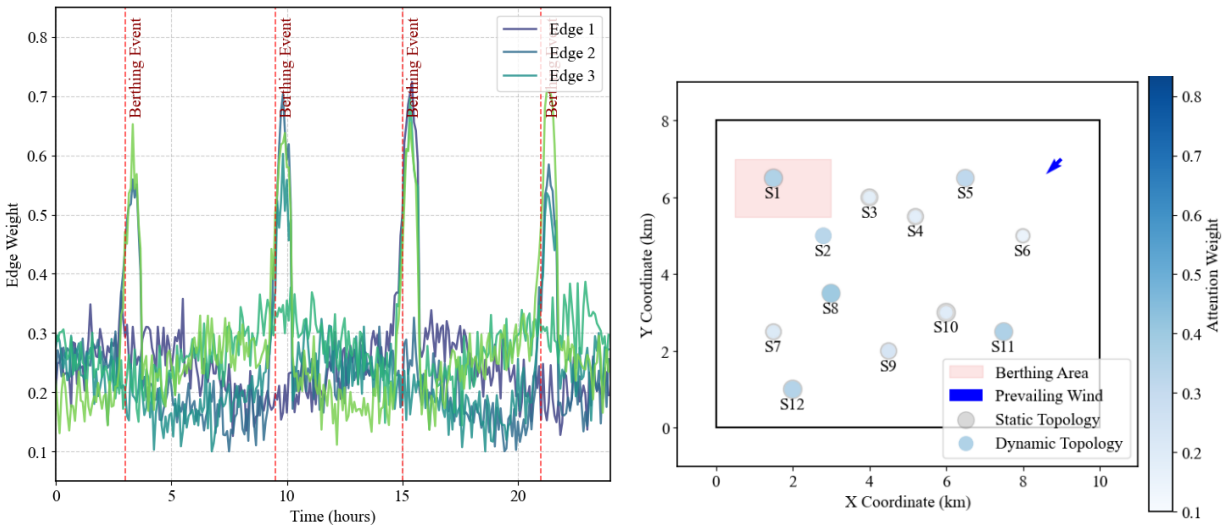

(a) Dynamic evolution of edge weights driven by ship activity (b) Static comparison and dynamic topological attention

Fig. 3. Spatiotemporal characteristics of dynamic topology mechanism

Fig. 3 shows the spatiotemporal characteristics of the dynamic topology mechanism. Sub-graph in fig. 3(a) with time series as the horizontal axis and edge weights as the vertical axis, reveals the dynamic evolution of key edge weights triggered by ship berthing events. The abrupt changes in edge weights at the four typical berthing events correspond to ship activities, and different edges show varying response amplitudes in the same event. Sub-graph in fig. 3(b) compares the attention distribution characteristics of static and dynamic topologies through port spatial layout visualization. Static topology does not show a clear spatial concentration trend. In dynamic topology, nodes in some areas are darker, indicating higher attention weights. The arrows in fig. 3 indicates the prevailing wind direction, and the weight distribution extends roughly along this direction, suggesting that dynamic correlations may be affected by wind direction.

This phenomenon originates from the adaptive topology-sensing approach developed in this paper, which creates an event-driven graph structure adaptive evolution framework by merging ship AIS trajectories and meteorological data in real time. When sudden events, such as a ship tying up, occur, the sudden event detection unit immediately activates the edge weight update algorithm to dynamically modify the adjacency matrix employing information about the ship's position, the emission intensity of the source, and the wind direction to enhance the time-dependent topological connection between the pollution source and the downwind station. This addresses the static nature of GCN-Att's traditional topology, allowing graph neural networks to isolate unique dynamic paths of pollution diffusion associated with ports. It allows rapid response times to abrupt events, accurately models spatial association, resolves the mismatch between dynamic pollution events and static port modelling, and provides theoretical support for high-precision air quality monitoring in complex environments.

3.3. Robustness Verification of Real-Time Monitoring Scenarios

To address the actual monitoring needs of ports under extreme weather conditions such as typhoons, this section systematically verifies the robustness of the proposed model from five aspects: response, fault tolerance for lost data, update frequency, energy consumption, and cross-port generalization error.

The comparison methods include: (1) Static GCN-Att, which uses a fixed adjacency matrix GCN-Att fusion model as the ablation baseline of the proposed method. (2) Dynamic Graph Neural Network (DGNN), which adaptively constructs an adjacency matrix based on historical monitoring data, but does not integrate AIS or meteorological information. (3) Spatio-

Temporal Transformer (ST-Transformer), which combines graph convolution and a multi-head self-attention mechanism into a spatiotemporal model with a static graph structure but strong temporal modelling ability. (4) Threshold-Adaptive Graph (TAG), which dynamically adjusts the station connection relationship according to a pre-set pollutant concentration threshold, representing a common heuristic mapping strategy in port monitoring. All baselines are retrained and tested on the same dataset and hardware environment to ensure the fairness of the comparison. All baseline models employed identical input feature dimensions and prediction horizons to ensure comparable evaluation metrics. Hyperparameters regarding learning rates and hidden layer dimensions remained consistent across all graph-based architectures to isolate the performance contribution of the dynamic topology module. The Spatio-Temporal Transformer uses the standard multi-head attention configuration without the dynamic adjacency matrix injection.

To simulate typhoon weather conditions, three sets of comparative experiments are designed: (1) the proportion of missing data is gradually increased (0%-50%), and the sudden change response latency is measured. (2) The model is run continuously for 72 hours, and the model update frequency and system energy consumption are recorded. (3) The trained model is transferred to three different ports to evaluate the cross-regional generalization ability. The results are shown in Table 3.

Table 3. Comparison of indicators between model and baseline methods under typhoon weather

Method	Response Latency (s)	Missing Data Tolerance (%)	Update Frequency (times/hour)	Energy Consumption (W·h/24h)	Cross-Port Generalization Error (MAE, μg/m³)
Static GCN-Att	15.3	60	0.5	39.8	7.1
DGNN	12.1	71	2.8	56.4	6
ST-Transformer	10.4	67	1.7	68.2	6.3
TAG	13.8	58	1.2	44.1	6.8
GCN-Att + Dynamic Topology	8.1	86	4.3	51.6	4.7

Table 3 compares the proposed method (GCN-Att + Dynamic Topology) with four baselines under typhoon disturbances across five robustness metrics. The proposed model, with a mutation response latency of 8.1 seconds, significantly outperforms baselines such as Static GCN-Att (15.3 seconds) and DGNN (12.1 seconds). Its data missing tolerance reaches 86%, surpassing other methods; it exhibits the lowest cross-port generalization error (MAE = 4.7 μg/m³), validating its transferability. Despite an update frequency of 4.3 times/hour, its energy consumption (51.6 W·h/24h) is still lower than ST-Transformer (68.2 W·h/24h), demonstrating a balance between dynamism and energy efficiency.

This paper presents a collaborative multi-source dynamic mapping approach that fuses AIS trajectory data with wind direction data to reconstruct an adjacency matrix in real time, update edge weights when sudden events are identified, such as docking, and to learn how pollution signals can propagate towards the actual diffusion path. Conversely, Static GCN-Att has a fixed topology; DGNN lacks physical drivers. TAG relies on threshold lag responses, and all are challenging to incorporate when predicting a rapidly changing pollution field due to storm fluctuations. Using multi-source, event-driven, collaborative mapping allows for faster, more accurate monitoring, enabling a better, more generalized response, even during extreme weather conditions.

4. Conclusion

In response to the modelling paradox of dynamic pollution events occurring in ports and static graph models, this research proposes a dynamic spatial adjacency matrix generated by a topological sensing GCN-Att fusion model by using ship AIS trajectories and meteorological data. The event-driven dynamic spatial adjacency matrix, in combination with a real-time edge-weight update mechanism that reacts to sudden events, and allows for the adaptive evolution of the graph structure to reflect the diffusion path of pollution. The results show a significant improvement in prediction accuracy in sudden event scenarios for ships berthing, a reduction in the time response to the sudden edge latency to 8.1 seconds for extreme disturbances, such as typhoons, the ability to tolerate 86% missing data in sudden disturbances, and a cross-port generalization error of only 4.7 μg/m³, demonstrating high accuracy, low latency, and robustness. Current reliance on AIS data streams limits model performance in signal-blind zones where trajectory continuity degrades. Future research targets integrating satellite remote sensing to mitigate terrestrial sensing blind spots and developing lightweight edge-computing frameworks to reduce data transmission latency.

Author Contributions

Shoubo Zhang contributed to conceptualization, methodology, investigation, data collection, analysis, draft preparation, manuscript editing, visualization, supervision, and project administration, and serves as the corresponding author. Pingwei Zhou contributed to methodology, investigation, data collection, analysis, and manuscript editing. Guannan Xu contributed to conceptualization, investigation, data collection, and supervision. Zongtao Mu contributed to investigation, data collection, analysis, and visualization. Dong Wang contributed to supervision, project administration, and manuscript editing. All authors have read and agreed with the manuscript before its submission and publication.

Funding

This research received no specific financial support from any funding agency.

Institutional Review Board Statement

Not applicable.

Declaration of AI Tools

The authors confirm that no Artificial Intelligence (AI) tools were used in the preparation of this manuscript.

References

Barberi, S., Sambito, M., Neduzha, L., and Severino, A. (2021). Pollutant Emissions in Ports: A Comprehensive Review. *Infrastructures*, 6(8), 114.

Benhaddi, M. and Ouarzazi, J. (2021). Multivariate Time Series Forecasting with Dilated Residual Convolutional Neural Networks for Urban Air Quality Prediction. *Arabian Journal for Science and Engineering*, 46(4), 3423-3442.

Campos, P.M., Esteves, A.F., Leitao, A.A., and Pires, J.C. (2021). Design of Air Quality Monitoring Network of Luanda, Angola: Urban Air Pollution Assessment. *Atmospheric Pollution Research*, 12(8), 101128Tseng, P. H. and Ng, M. W. (2021). Assessment of Port Environmental Protection in Taiwan. *Maritime Business Review*, 6(2), 188-203.

Garbatov, Y. and Georgiev, P. (2022). Air Pollution and Economic Impact from Ships Operating in the Port of Varna. *Atmosphere*, 13(9), 1526.

Geng, X., Li, Y., and Sun, Q. (2023). A Novel Short-Term Ship Motion Prediction Algorithm Based on EMD and Adaptive PSO – LSTM With the Sliding Window Approach. *Journal of Marine Science and Engineering*, 11(3), 466.

Gu, J., Jia, Z., Cai, T., Song, X., and Mahmood, A. (2023). Dynamic Correlation Adjacency-Matrix-Based Graph Neural Networks for Traffic Flow Prediction. *Sensors*, 23(6), 2897.

Han, J., Liu, H., Xiong, H., and Yang, J. (2022). Semi-Supervised Air Quality Forecasting via Self-Supervised Hierarchical Graph Neural Network. *IEEE Transactions on Knowledge and Data Engineering*, 35(5), 5230-5243.

Islam, M.A., Ahmed, C.F., Alam, M.T., and Leung, C.K.S. (2024). Graph-Based Substructure Pattern Mining with Edge-Weight. *Applied Intelligence*, 54(5), 3756-3785.

Jia, H., Yang, Y., An, J., and Fu, R. (2023). A Ship Trajectory Prediction Model Based on Attention-BILSTM Optimized by the Whale Optimization Algorithm. *Applied Sciences*, 13(8), 4907.

Johnson, M.T., Arif, I., Marchetti, F., Munshi-South, J., Ness, R.W., Szulkin, M., Verrelli, B.C., Yauk, C.L., Anstett, D.N., Booth, W., and Caizergues, A.E. (2024). Effects of Urban-Induced Mutations on Ecology, Evolution and Health. *Nature Ecology & Evolution*, 8(6), 1074-1086.

Jun, W., Tianliang, Z., Jiahui, Z., Tianyi, L., and Chunzhi, W. (2023). Hierarchical Multiples Self-Attention Mechanism for Multi-Modal Analysis. *Multimedia Systems*, 29(6), 3599-3608Santos, T. A. (2025). Sustainable Port Operations: Pollution Prevention and Mitigation Strategies. *Sustainability*, 17(11), 4798.

Kim, H., Bui, H. D., and Hong, S. (2022). Estimation of Air Pollution from Ships in Port Area: A Case Study of Yeosu and Gwangyang Ports in Korea. *Atmosphere*, 13(11), 1890.

Lee, H.T., Lee, J.S., Yang, H., and Cho, I.S. (2021). An AIS Data-Driven Approach to Analyze the Pattern of Ship Trajectories in Ports Using the DBSCAN Algorithm. *Applied Sciences*, 11(2), 799.

Li, M., Li, B., Qi, Z., Li, J., and Wu, J. (2024). Enhancing Maritime Navigational Safety: Ship Trajectory Prediction Using ACoAtt – LSTM and AIS Data. *ISPRS International Journal of Geo-Information*, 13(3), 85.

Li, P., Zhang, T., and Jin, Y. (2023). A Spatio-Temporal Graph Convolutional Network for Air Quality Prediction. *Sustainability*, 15(9), 7624.

Li, X. (2024). A Faster Deep Graph Clustering Network Based on Dynamic Graph Weight Update Mechanism. *Cluster Computing*, 27(9), 12123-12140.

Li, X.Z., Peng, Z.R., Fu, Q., Wang, Q., Pan, J., and He, H. (2024). A Data-Driven Approach to Identify Major Air Pollutants in Shanghai Port Area and Their Contributing Factors. *Journal of Marine Science and Engineering*, 12(2), 288.

Liang, Q., Xie, D., Dong, Z., Li, H., Li, H., Gadway, B., Yi, W., and Yan, B. (2022). Dynamic Signatures of Non-Hermitian Skin Effect and Topology in Ultracold Atoms. *Physical Review Letters*, 129(7), 070401.

Liu, H., Han, Q., Sun, H., Sheng, J., and Yang, Z. (2023). Spatiotemporal Adaptive Attention Graph Convolution Network for City-Level Air Quality Prediction. *Scientific Reports*, 13(1), 13335.

Malek, M. R. (2023). Spatial Analysis in Curved Spaces With Non-Euclidean Geometry. *Journal of Geomatics Science and Technology*, 12(2), 167-175.

Motlagh, N.H., Kortoçi, P., Su, X., Lovén, L., Hoel, H.K., Haugsvær, S.B., Srivastava, V., Gulbrandsen, C.F., Nurmi, P., and Tarkoma, S. (2023). Unmanned Aerial Vehicles for Air Pollution Monitoring: A Survey. *IEEE Internet of Things Journal*, 10(24), 21687-21704.

Pan, C., Zhu, J., Kong, Z., Shi, H., and Yang, W. (2021). DC-STGCN: Dual-Channel Based Graph Convolutional Networks for Network Traffic Forecasting. *Electronics*, 10(9), 1014.

Pan, J., Wang, Y., Qin, X., Gali, N.K., Fu, Q., and Ning, Z. (2024). Spatiotemporal Analysis of Complex Emission Dynamics in Port Areas Using High-Density Air Sensor Network. *Toxics*, 12(10), 760.

Ren, X., Zhao, K., Riddle, P.J., Taskova, K., Pan, Q., and Li, L. (2023). Damr: Dynamic Adjacency Matrix Representation Learning for Multivariate Time Series Imputation. *Proceedings of the ACM on Management of Data*, 1(2), 1-25.

Sembiring, I., Manongga, D., Rahardja, U., and Aini, Q. (2024). Understanding Data-Driven Analytic Decision Making on Air Quality Monitoring: An Empirical Study. *Aptisi Transactions on Technopreneurship (ATT)*, 6(3), 418-431.

Shi, Z., Zhang, M., Han, M., Zhang, Y., Ma, G., and Ren, H. (2024). BresNet: Applying Residual Learning in Backpropagation Neural Networks to Predict Ground Surface Concentration of Primary Air Pollutants. *Remote Sensing*, 16(16), 2897.

Sun, Y., Zhang, J., Zhang, Y., Yu, L., Yuan, Z., Liu, G., and Wang, Q. (2022). Environment Features-Based Model for Path Loss Prediction. IEEE Wireless Letters, 11(9), 2010-2014.

Tai, H. H. and Wang, Y. M. (2022). Influence of Vessel Upsizing on Pollution Emissions Along Far East – Europe Trunk Routes. Environmental Science and Pollution Research, 29(43), 65322-65333.

Wang, J., Liao, N., Du, X., Chen, Q., and Wei, B. (2024). A Semi-Supervised Approach for the Integration of Multi-Omics Data Based on Transformer Multi-Head Self-Attention Mechanism and Graph Convolutional Networks. *BMC Genomics*,

Wang, Y., Liu, K., He, Y., Wang, P., Chen, Y., Xue, H., Huang, C., and Li, L. (2024). Enhancing Air Quality Forecasting: A Novel Spatio-Temporal Model Integrating Graph Convolution and Multi-Head Attention Mechanism. *Atmosphere*, 15(4), 418.

Ye, Y. and Geng, P. (2023). A Review of Air Pollution Monitoring Technology for Ports. *Applied Sciences*, 13(8), 5049.

Zhou, F., Liu, J., Zhu, H., Yang, X., and Fan, Y. (2022). A Real-Time Measurement-Modeling System for Ship Air Pollution Emission Factors. *Journal of Marine Science and Engineering*, 10(6), 760.

Shoubo Zhang, Deputy Manager and Safety Director at First Stevedoring Branch Company, SPG Rizhao Port Group Co., Ltd. His research focuses on port equipment management and environmental protection management. He is deeply involved in the construction of Chin''s intelligent green demonstration ports for bulk dry cargo, and is committed to building green, low-carbon smart ports, continuously exploring new technological practices such as intelligent dust suppression in bulk cargo yards, automated dry bulk cargo yards, and establishing a comprehensive, procedural, and multi-dimensional port environmental management system. This has significantly improved environmental protection in the port area and achieved harmonious coexistence between the port and the city.

Pingwei Zhou holds a master's degree and is currently in the First Stevedoring Branch Company, SPG Rizhao Port Group Co., Ltd., and serves as a deputy manager. His research interests are in green transformation and environmental protection innovation of port equipment. Focuses on the green transformation and application of environmental protection technologies in port operation equipment. He participates in projects such as promoting electric port machinery, constructing ship shore power systems, and developing emission-monitoring platforms for port operation machinery, promoting the application of new energy and clean technologies in port equipment. Aims to build a green port equipment system and support the low-carbon transformation of ports.

Guannan Xu is the Deputy Director of the Technology Innovation Center, SPG Rizhao Port Group Co., Ltd. His research interests are in automation and unmanned operations in terminals. He is deeply involved in the research and development of multiple automated systems, including the intelligent scheduling system for bulk dry bulk cargo terminals, the automated rail-mounted gantry crane scheduling system for container terminals, the unmanned container truck intelligent scheduling system, and the remote-controlled quay crane operation system.

Zongtao Mu, a Deputy Department Manager in Technology Innovation Center, SPG Rizhao Port Group Co., Ltd. His research interests include the Intelligence of Port Environmental Monitoring Systems and Equipment. Dedicated to the intelligent upgrade and system integration of port environmental monitoring equipment. Deeply involved in the construction of an online air pollution monitoring network for ports and the research and development of intelligent dust monitoring and dust suppression linkage control systems. Promotes intelligent linkage and closed-loop control between environmental monitoring equipment and port operation equipment, enhancing the precision and automation of port environmental governance.

Dong Wang, Executive Director in Shandong Port Technology Group Rizhao Co., Ltd. His research interests include port information and intelligence. Committed to the research on port production operation information and the intelligence of production operations. He is deeply involved in the development of integrated service platforms, including the "Zhoudao Network" port supply chain platform and the intelligent bulk dry bulk cargo yard system. Aims to realize the digital transformation and ecological development of ports.